Molecular Therapy
Nucleic Acids
Original Article

Biologically stable threose nucleic acid-based probes for real-time microRNA detection and imaging in living cells

Fei Wang,[1] Ling Sum Liu,[1] Pan Li,[1] Hoi Man Leung,[1] Dick Yan Tam,[1] and Pik Kwan Lo[1,2]

[1]Department of Chemistry, City University of Hong Kong, Tat Chee Avenue, Kowloon Tong, Hong Kong SAR, China; [2]Key Laboratory of Biochip Technology, Biotech and Health Care, Shenzhen Research Institute of City University of Hong Kong, Shenzhen 518057, China

We successfully fabricated threose nucleic acid (TNA)-based probes for real-time monitoring of target miRNA levels in cells. Our TNA probe is comprised of a fluorophore-labeled TNA reporter strand by partially hybridizing to a quencher-labeled TNA that is designed to be antisense to a target RNA transcript; this results in effective quenching of its fluorescence. In the presence of RNA targets, the antisense capture sequence of the TNA binds to targeted transcripts to form longer, thermodynamic stable duplexes. This binding event displaces the reporter strand from the quencher resulting in a discrete "turning-on" of the fluorescence. Our TNA probe is highly specific and selective toward target miRNA and is able to distinguish one to two base mismatches in the target RNA. Compared with DNA probes, our TNA probes exhibited favorable nuclease stability, thermal stability, and exceptional storage ability for long-term cellular studies. Our TNA probes are efficiently taken up by cells with negligible cytotoxicity for dynamic detection of target miRNAs and can also differentiate the distinct target miRNA expression levels in different cell lines. This work illuminates for using TNA as a building component to construct a biocompatible probe for miRNA detection that offers alternative molecular reagents for miRNA-related diagnostics.

INTRODUCTION

MicroRNAs (miRNAs), a class of small non-coding RNA molecules of approximately 21–23 nucleotides in length, regulates the post-transcriptional gene expression via selective messenger RNA (mRNA) silencing.[1,2] Altered expression of miRNAs leads to pathological progression because various biological activities, including cell proliferation, differentiation, and apoptosis, are associated with miRNAs.[3] Thus, the expression of certain miRNAs is considered a potential biomarker in the diagnosis and prognosis of diseases; for example, cancer. Conventional techniques for miRNA analysis in homogeneous solutions, such as quantitative reverse transcription polymerase chain reaction (qRT-PCR), northern blotting, microarrays, and next-generation sequencing (NGS), have been widely used.[4,5] However, these analytical methods still have shortcomings that seriously hamper their practical applications. For instance, complex RNA extraction steps are involved in detecting relative miRNA in bulk samples. The pooling of miRNA from cell lysates makes it incapable of real-time monitoring of target miRNA levels *in situ* for clinical diagnosis and research laboratories. Particularly, longer time-to-result and large quantity of samples are required for northern blotting with low sensitivity and throughput. Although qRT-PCR exhibits high sensitivity and accuracy, large amounts of designed primers and precise temperature control for amplification are required, which increase its experimental costs and analytical complexity. Moreover, the limitations of microarray and NGS techniques are poorly reproducible and back-end informatics, respectively. Currently, direct imaging of miRNA in living cells is very limited in how it provides a valuable means for identifying cancerous cells and evaluating drug efficacy in real time.[2,6,7] Thus, it is imperative to develop rapid, convenient, cost-effective, and sensitive approach for *in situ* detection of miRNA expression at the single-cell level.

Due to the flexibility offered by natural nucleic acids, hybridization-based probes that are designed to leverage Watson-Crick base pairing for detecting complementary nucleic acid sequences have recently become hotspots in endogenous miRNA detection research.[8,9] The recognition nucleic acid strands are usually functionalized with fluorescence resonance energy transfer pair, fluorescent dye quencher pairs, or intercalator dye of the thiazole orange family to form a molecular beacon for fluorescence analysis upon target binding.[10,11] To facilitate signal amplification, recognition nucleic acid strands are further integrated into a large variety of nanomaterials, including nanoparticles, liposomes, polymers, manganese dioxide nanosheet, graphene oxide, quantum dots, and self-assembled DNA nanostructures, as intracellular probes for live cells and/or tissues.[9] Nonetheless, challenges, such as enzymatic degradation, nuclear sequestration, high false-positive signal, cytotoxicity, and the demand for transfection agents, remain concerning their development into viable diagnostic systems.[12–14] To improve the applicability, xeno nucleic acids (XNAs), which are chemically modified nucleic acid analogs, such

Received 3 October 2021; accepted 31 December 2021;
https://doi.org/10.1016/j.omtn.2021.12.040.

Correspondence: Pik Kwan Lo, Department of Chemistry, City University of Hong Kong, Tat Chee Avenue, Kowloon Tong, Hong Kong SAR, China.
E-mail: peggylo@cityu.edu.hk

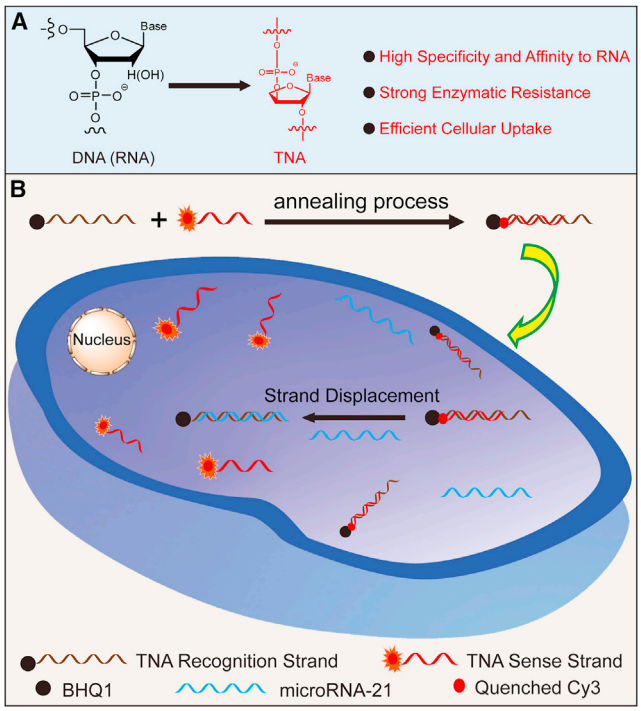

Figure 1. Design of the TNA-based probes

(A) Chemical structures of DNA (or RNA), TNA polymers, and the attractive characteristics of TNA. (B) Schematic illustration of the preparation of TNA-based probes for miRNA detection and imaging. The short Cy3-TNA sense strands are released via the displacement process upon binding of miR-21 to the BHQ1-TNA recognition strands, resulting in the recovery in fluorescence.

as locked nucleic acid (LNA),[15] peptide nucleic acid,[16,17] and 2′ O-methyl RNA,[13] have been used as building blocks to construct biosensors to detect endogenous RNAs in living cells. Compared with DNA-based probes, these chemically modified nucleic acid analog-based probes exhibit high thermal stability and strong binding affinity and specificity toward target RNAs, resulting in shorter detection time and lower detection limits in the femtomolar scale. However, the exploration of XNA-based RNA detection techniques is still limited. Only miRCURY LNA miRNA Detection Probes are commercially available from QIAGEN (USA). Some disadvantages of these LNA-based biosensors have been raised from the several sequence limitations in the synthesis of this nucleic acid analog. In particular, the design of LNA oligomers is constrained by four requirements: (1) sequences of more than four LNA nucleotides must be circumvented; (2) sequences of three or more Cs or Gs must be prevented; (3) the GC content must be restricted between 30% and 60%; and (4) self-complementarity or cross-hybridization must be avoided. These limitations in the sequences of LNA oligomers that can be synthesized and used as capture probes in biosensors can markedly impair the detection of some mutations in genes of interest. Thus, the commercially available LNA-based probes are not high-throughput biosensors with widespread applicability in biotechnology or in the clinical setting.[18]

Recently, (3′,2′)-α-L-TNA (Figure 1A), in which the five-carbon ribose in DNA is replaced by the four-carbon threose, has attracted extensive attention as an alternative genetic material.[19–21] Despite the one-atom shorter sugar-phosphate backbone, TNA still possesses the capability to adopt stable antiparallel duplexes with complementary strands of DNA, RNA, and itself in a sequence-dependent manner via Watson-Crick base pairing.[19,22,23] Due to its chemical simplicity, its unique ability to exchange genetic information with RNA, and the ability to fold into tertiary structures, TNA has been considered as a potential progenitor of RNA.[22,24] Up to now, enormous efforts have been devoted to the efficient and faithful biological or chemical synthesis of TNA polymers,[25–28] which has boosted investigation of TNA in the fields of aptamer discovery,[22,29–32] XNAzyme development,[33–35] nucleic acid therapeutics,[28,36–38] gene delivery,[39] and information storage.[40] For example, Yu and coworkers reported a selection of TNA aptamers that effectively bind PD-L1 protein and inhibit the PD-1/PD-L1 interaction. Subsequently, they demonstrated that intravenous administration of TNA aptamer N5 can specifically accumulate at a tumor site and remarkably suppress its growth with negligible side effects.[38] Wang et al. demonstrated that the introduction of TNA and 2′-deoxy-2′-fluoro-β- D -arabinonucleic acid (FANA) modifications into a classical DNAzyme 10–23 (X10-23) significantly enhanced the biological stability and catalytic activity. The modified X10-23 resulted in efficient and persistent gene-silencing activity via the degradation of mRNA molecules in cultured mammalian cells.[33] In addition, Ding and coworkers proposed a strategy for the construction of a terminal-closed linear gene with a TNA loop-modified primer pair through PCR. The developed linear gene had enhanced enzymatic resistance and serum stability, and elicited a potent and persistent EGFP gene expression in eukaryotic cells.[39] The superior characteristics of strong physiological stability, high specificity and affinity toward cDNA or RNA, strong enzymatic resistance, and efficient cellular uptake makes TNA a promising candidate for the development of a new generation of biologically stable XNA-based biosensors for biomedical applications.[37,41]

In this study, we examined, for the first time, the feasibility of using TNA as a building component to construct a biocompatible probe for rapid and selective fluorescence detection and imaging of intracellular RNA targets (Figure 1B). This TNA-based probe is comprised of a fluorophore-labeled TNA reporter strand by partially hybridizing to a quencher-labeled TNA oligonucleotide, which is designed to be antisense to a target RNA transcript via pair pairing. Hybridization of the reporter sequence holds the fluorophore in close proximity to the quencher, effectively quenching its fluorescence. Upon cellular entry, without the need for harmful transfection treatment, the antisense capture sequence of the TNA binds to targeted transcripts and form longer and thermodynamic stable duplexes. These target binding events displace the reporter strand from the quencher, resulting in a discrete "turning-on" of the fluorescence. The extent of fluorescence enhancement is quantifiably related to the target RNA expression level. In addition, this TNA probe can be rapidly detected, has

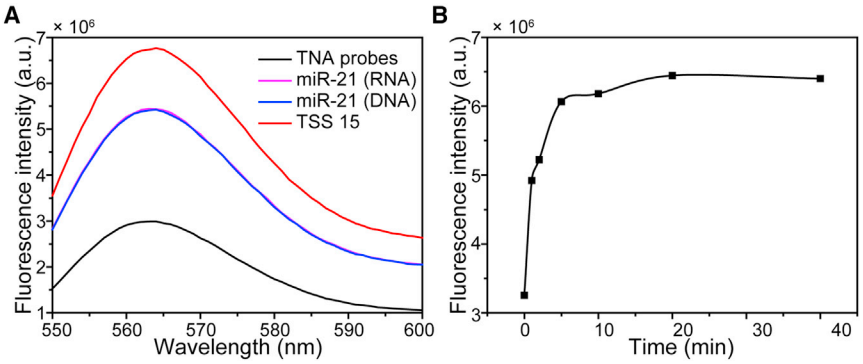

Figure 2. Characterization of designed TNA probes
(A) The fluorescence spectra of Cy3-labeled TSS, and TNA probes before and after incubation of miR-21 targets. (B) The fluorescence intensities change of TNA probes at 564 nm after addition of miR-21 as a function of incubation time.

excellent selectivity and specificity toward target miRNAs and is able to distinguish the target molecules with one to two base mismatches. Compared with DNA probes, the superior nuclease and thermal stability, in addition to the excellent long-term storage stability, make TNA probes biocompatible and cost-effective biosensors for dynamic real-time imaging of target miRNA expression in living cells. This work contributes significantly to a new generation of biocompatible xeno nucleic acid-based biosensors for identifying cancerous cells and real-time evaluation of drug efficacy.

RESULTS

Design of TNA probes for miRNA detection

The TNA oligonucleotides used in this study were synthesized in accordance with the previously established solid-phase synthetic protocol shown in Figure S1 (the detailed experimental procedure is provided in the supplemental information). The synthetic TNA and DNA oligonucleotides with designed sequences were confirmed by matrix-assisted laser desorption/ionization time-of-flight mass spectrometry (MALDI-TOF) and denaturing polyacrylamide gel electrophoresis (PAGE) analysis as shown in Table S1, and Figures S2 and S3.

The assay strategy is illustrated in Figure 1B. The TNA probes were constructed by partial hybridization of a 2′-Black Hole Quencher 1 (BHQ1)-labeled TNA recognition strand (TRS) with a 3′-Cy3-labeled TNA sense strand (TSS). The sequence of TRS is antisense to a target microRNA-21 (miR-21), which is a key regulatory molecule overexpressed in various cancer cells for tumor initiation and progression.[42] In the absence of target miRNA, the fluorescence signal of Cy3 is very weak and difficult to detect due to the quenching effect of BHQ1, which is in close proximity to Cy3. In the presence of the target miRNA, the Cy3-labeled TSS is displaced by the target molecule and is then dissociated from the BHQ1-labeled TRS. Meanwhile, the TRS is fully hybridized with its complementary target miR-21 to form a thermodynamically stable complex. These binding events separate the BHQ1 and Cy3 fluorophore, resulting in the recovery of the Cy3 fluorescence signal. The extent of fluorescence enhancement is quantifiably related to the expression level of the target miRNAs. To achieve the maximum quenching effect between Cy3 and BHQ1 before target binding, the fluorescence spectra of the TNA probe comprised of 22-mer TRS and TSS with different number of nucleobases (11-mer, 13-mer, and 15-mer) were measured and compared. As shown in Figure S4, the TNA probe comprised of TRS and TSS 15 achieved the best quenching effect with a reduction of 50%. Thus, TRS and TSS 15 were selected to form the duplex TNA-based probe for future study. As a control, scrambled TNA probes were constructed from corresponding TNA duplexes.

Target recognition and detection

To verify the detection strategy, we measured the fluorescence intensity of duplex TNA-based probes in phosphate-buffered saline (PBS) buffer before and after incubation with the same number of moles of target miR-21 for 40 min at 37°C. The Cy3 fluorescence signal in solution increased by 80% after miR-21 was added (Figure 2A). In contrast, fluorescence from the scrambled TNA probes incubated with miR-21 was negligible indicating that the strand displacement reaction is sequence dependent (Figure S5). Interestingly, any DNA or RNA analogs achieved similar fluorescence recovery, strongly suggesting that the sugar conformation of the target molecules does not affect target recognition. Considering the relatively high cost and poor enzymatic resistance of RNA molecules, miR-21 DNA mimics were subsequently used for *in vitro* detection assays. To further optimize the detection kinetics, we evaluated the displacement reaction kinetics of the designed TNA probes by measuring the Cy3 fluorescence intensities of the TNA probe at different time points after the addition of equivalent moles of target miR-21. The Cy3 fluorescence increased for ~10 min before reaching a plateau corresponding to the complete strand displacement reaction as shown in Figure 2B. Native PAGE analysis also confirmed the formation of different components after the strand displacement reaction in these binding events. As shown in Figure S6A, a band in lane 4 with the slowest mobility was observed for the TRS/TSS duplexes (TNA probe). In contrast, after adding miR-21 mimics into the well-formed TRS/TSS duplex probes a new band was observed in lane 6 with higher mobility, which is equivalent to the TRS/miR-21 complexes in lane 5. In addition, a strong Cy3 signal in lane 6 was observed, which was equivalent to free TSS 15 in lane 2. The diffusion of the bands was due to the prolonged electrophoresis in native PAGE. We conducted an additional native PAGE experiment with a shorter running time (6 h), and we still observed the fluorescence recovery (Figure S6B). However, the altered mobilities of the bands were not obvious. These results confirmed the formation of TRS/miR-21 duplexes and the dissociation of TSS 15 from TRS during the strand displacement reaction.

Specificity and sensitivity for target miRNA detection

The TNA probe was further evaluated *in vitro* for its utility in quantifying complementary miRNA targets in a sequence-specific

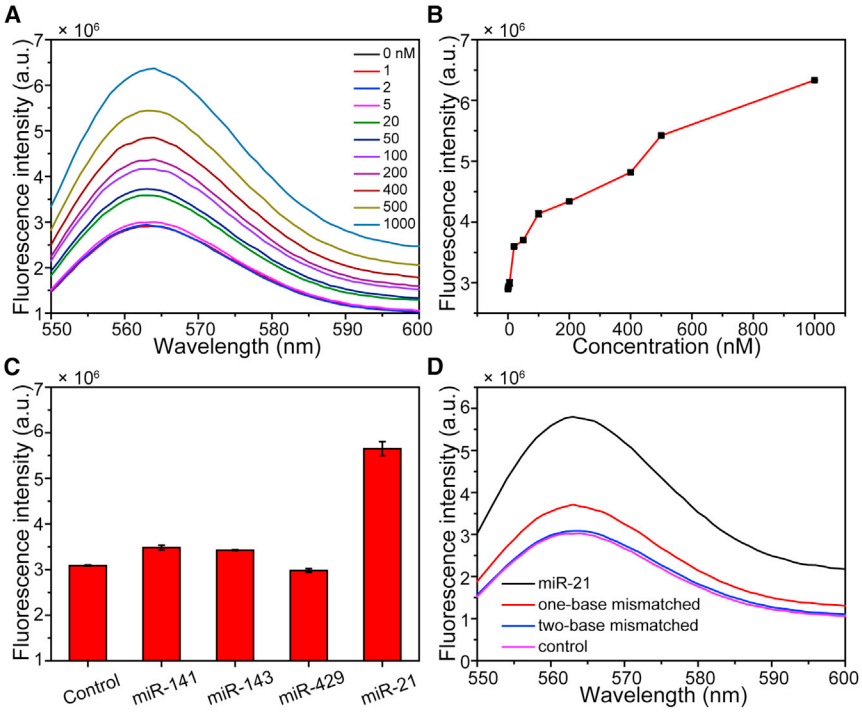

Figure 3. TNA probes for *in vitro* detection of miR-21

(A) Fluorescence spectra and (B) corresponding titration curve of TNA probes after addition of miR-21 targets at various concentrations. (C) The fluorescence intensities of TNA probes at 564 nm before (as control) and after incubating of miR-21 targets and three control miRNA mimics, including miR-141, miR-143, and miR-429. (D) The fluorescence spectra of TNA probes before (as control) and after incubation with miR-21 targets, and the miR-21 targets with one or two bases mismatched.

manner. Solutions of duplex TNA-based probes (500 nM) were examined before and after adding 1–1,000 nM miR-21 in PBS buffer for 40 min at 37°C. As indicated in Figures 3A and 3B, upon addition of the target RNA, Cy3 fluorescence increased as miR-21 concentrations increased. Therefore, fluorescence activation correlated with the concentration of target RNAs. Figure S7 shows a linear correlation between target miR-21 (0–20 nM) and fluorescence peak intensities at 564 nm (r^2 = 0.99). It should be noted that similar results with slope changes between different concentration ranges have also been reported in other publications centered on miRNA detection systems.[7,43–45] According to Xing and coworkers, a prozone effect occurs when the concentration of targets is relatively high, and that the fluorescence signal does not increase linearly with increasing target concentration.[43] The limit of detection was calculated to be 2.582 nM according to 3σ/κ (where σ is the standard deviation of blank measurements and κ is the slope), which is comparable with the previously reported methods for miRNA detection.[46,47]

To investigate the specificity, 500 nM of the control miRNA mimics (miR-141, miR-143, and miR-429) were added into the TNA probes in PBS buffer. Compared with target miR-21, negligible changes of fluorescence intensity at 564 nm were observed (Figure 3C). The selectivity of the designed TNA probe was also evaluated by comparing the fluorescence signal generated by the miR-21 target with those containing one or two mismatched sequences. Figure 3D shows that the TNA probes exhibited a distinct difference in fluorescence enhancement toward the target miR-21 and a target miR-21 with one or two base mismatches. This indicates excellent selectivity of the designed TNA probes and their capability to distinguish base mismatches in target RNA molecules.

Biological stability of detection probes made of TNAs and DNAs

To investigate the stability of TNA, the nuclease stability of TRS/TSS duplexes was investigated to prevent this TNA probe from being destroyed within living cells. The TNA and corresponding DNA probes were incubated separately in PBS buffer containing 10% fetal bovine serum (FBS) for different durations, and the fluorescence peak intensity at 564 nm was subsequently measured before and after addition of target miR-21 (Figures 4A and 4C). The mixture of TNA probe and FBS did not significantly change fluorescence signals at 564 nm as a function of incubation time up to 24 h, indicating that TNA probes are excellent at protecting nuclease cleavage. When target miR-21 was added to the FBS-treated TNA probes, the fluorescence signals enhanced significantly and at similar intensities at various time points after hybridization proving that the fluorescence recovery was due to the target binding instead of nuclease degradation. These results strongly suggest that the FBS-treated TNA probes are still intact before target binding. In contrast, the rapid enhancement of fluorescence intensity at 564 nm of DNA probes after 2 h FBS treatment is attributed to the enzymatic degradation of DNA probes prior to target miRNA binding. Denaturing PAGE analysis shown in Figures 4B and 4D further confirmed no degradation of TNA probes after FBS treatment for 24 h. These results are highly consistent with our reported studies.[37] However, rapid digestion of DNA probes was observed upon FBS treatment with a calculated half-life of 1.35 h (Figure S8). Detailed calculations are provided in supplemental information. The enzymatic resistance assays clearly demonstrate that the DNA-based probes suffer from poor enzymatic resistance and exhibit a false-positive signal in physiological conditions. We also investigated the influence of temperature change on the TNA probes. As shown in Figure 4E, the TNA probes are insensitive to temperature demonstrated by less variations at fluorescence intensity at 564 nm compared with DNA probes upon temperature elevation. Furthermore, the long-term storage stability of TNA probes was studied by measuring the time-dependent Cy3 fluorescence intensity after incubation at 4°C. There was negligible change in

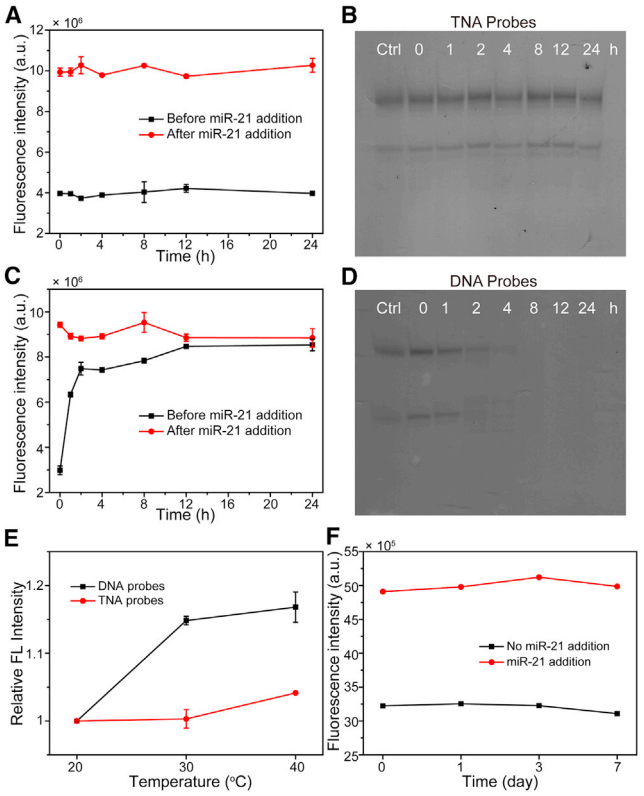

Figure 4. Stability of TNA probes

Fluorescence intensities of (A) FBS-treated TNA probes and (C) FBS-treated DNA probes before and after addition of miR-21 at designated time intervals (0, 1, 2, 4, 8, 12, and 24 h). Denaturing PAGE analysis of (B) TNA probes and (D) DNA probes against nuclease digestion incubated in FBS assay at various time intervals. Lane 1: control probes without FBS incubation and probes incubated with FBS for 0 h (lane 2); 1 h (lane 3); 2 h (lane 4); 4 h (lane 5); 8 h (lane 6); 12 h (lane 7); 24 h (lane 8). (E) The relative fluorescence intensities of detection probes made of DNAs and TNAs at 564 nm as a function of temperatures. (F) The fluorescence intensities of TNA probes at 4°C as a function of time before and after miR-21 addition.

fluorescence signals when stored for up to 7 days (Figure 4F, black curve). On the other hand, the TNA probe maintained its capability for target detection with enhanced fluorescence signals upon addition of miR-21 (Figure 4F, red curve), indicating long-term stable duplex hybridization of TNA probes.

miRNA imaging in living cells

Fluorescence imaging is a real-time, non-invasive, and radiation-free strategy that is widely used in medical diagnosis.[48] TNA oligonucleotides has been reported to internalize and accumulate in cells via a temperature- and energy-dependent endocytic mechanism.[28,37] Encouraged by the outstanding miRNA detection performance in solution and excellent stability in physiological conditions, we further investigated the miRNA sensing and imaging by TNA probes in living cells. To study the cytotoxicity of TNA duplexes, a standard 3-(4,5-dimethylthiazol-2-yl)-2,5-diphenyltetrazolium bromide (MTT) assay was used. As shown in Figure 5A, the relative cell viability of HEK293 normal cells and HeLa cancer cells remained at ~100% even after TNA incubation for 48 h, indicating excellent biocompatibility of TNA polymers. Afterward, the fluorescence response for miR-21 in HeLa cells was investigated and imaged using confocal laser scanning microscopy (CLSM). Time-dependent confocal fluorescence imaging showed that the intracellular fluorescence signal was observed after 6 h incubation and gradually increased with incubation time (Figures 5B and S9), confirming its applicability in the cellular environment for at least 24 h. We also studied the time-dependent dynamics of miRNA imaging via colocalization CLSM imaging. As shown in Figure S10, the fluorescence signal was not detected in the HeLa cells after 2 h incubation because TNAs accumulated inside the endosomes or lysosomes where target miRNAs are absent. The intracellular fluorescence signal gradually increased as the TNA probes escaped from the endosome/lysosome. Since the TNA probes did not degrade in the presence of enzymes, we confirm that the intracellular fluorescence signal was due to the responsiveness of TNA probes to the miR-21 target inside the cells.

We then investigated the capability of TNA probes in the evaluation of the relative expression levels of miR-21 in different cell lines. The HEK293 cell line with minimal expression of miR-21 was selected as a negative cell line and HeLa cancer cells with high expression of miR-21 were selected as a positive cell line. As shown in Figure 5C, differing fluorescence signal brightness was observed in the two different cell lines. HeLa cells had much higher fluorescence signals compared with HEK293 cells after incubation with miR-21-targeting TNA probes (in red color), indicating the upregulated expression of miR-21 in HeLa cells. These results were consistent with the previously reported varying expression levels of miR-21 in these two cell lines.[49] In addition, we performed an additional confocal fluorescence imaging experiment in which the HeLa and HEK293 cells were also incubated with scrambled TNA probes. As shown in Figure S11, HEK293 cells showed insignificant differences upon the incubation of scrambled probes and miR-21 targeting TNA probes. HeLa cells that were incubated with miR-21-targeting TNA probes displayed remarkably enhanced fluorescence intensity compared with cells incubated with scrambled probes. These data confirmed that the differing response of HEK293 and HeLa cells to the developed TNA probes is due to the differential expression of miR-21. Furthermore, we further evaluated the potential of TNA probes to detect the dynamic change of miR-21 expression levels in cells. HeLa cells were first transfected with anti-miR-21 to suppress their miR-21 expression level and then incubated with TNA probes for imaging. As shown in Figure 5D, very weak fluorescence signals were observed in the TNA probe-treated HeLa cells after anti-miR-21 transfection compared with non-transfected control cells.

DISCUSSION

miRNAs are considered to be molecular biomarkers in disease diagnosis and prognosis due to their participation in many biological activities.[2] Developing rapid and sensitive methods for the detection and imaging of miRNAs in living cells has received tremendous interest. In particular, significant advances have been achieved with

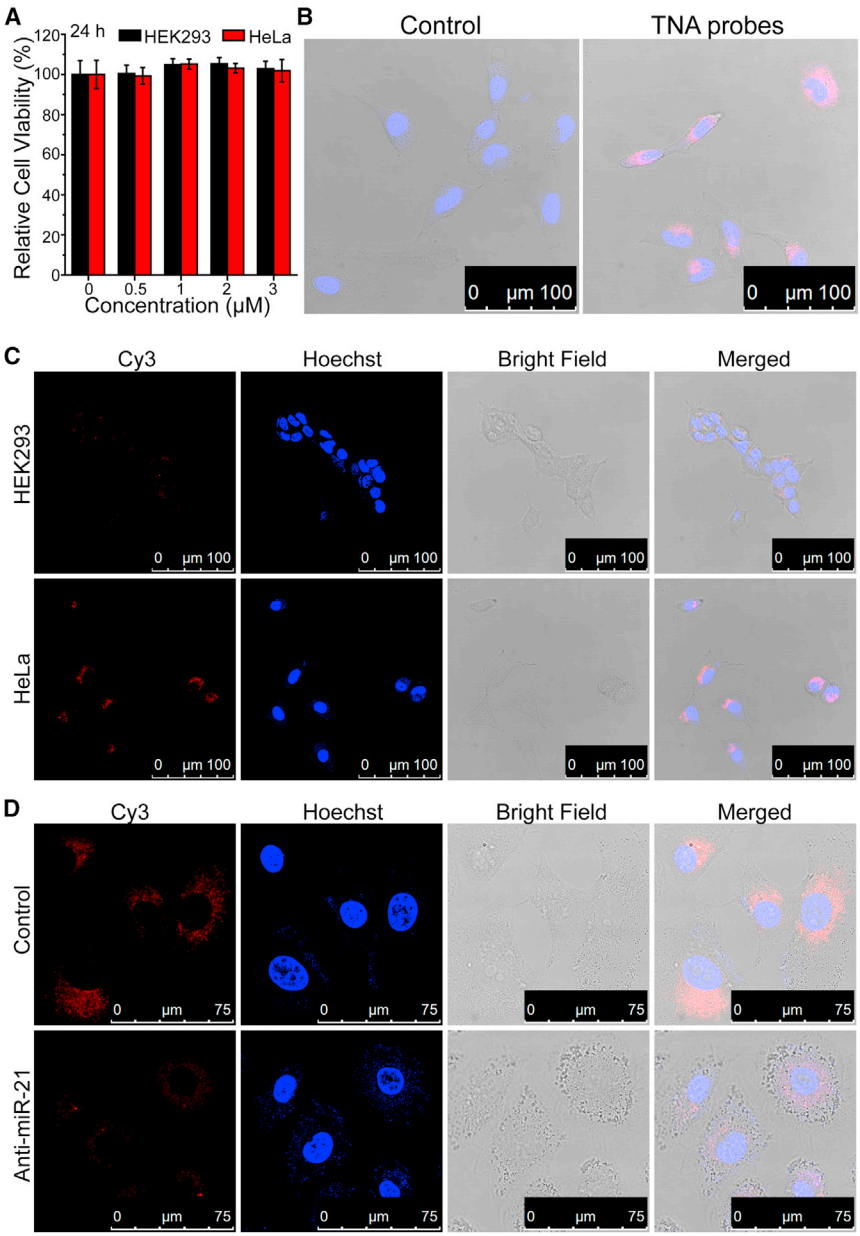

Figure 5. TNA probes for miR-21 imaging in live cells

(A) Relative cell viability of HEK293 and HeLa cells incubated with TNA duplexes for 24 h determined via MTT assays. Error bars indicate standard deviation (n = 6). (B) CLSM images of HeLa cells incubated with or without TNA probes for 24 h. Scale bar, 100 μm. (C) CLSM images of TNA probe-treated HEK293 cells and HeLa cells after incubation for 24 h. Scale bar, 100 μm. (D) CLSM images of TNA probe-treated HeLa cells (control) and HeLa cells transfected with anti-miR-21, followed by incubation of TNA probes for 24 h. Scale bar, 75 μm.

endogenous miRNA in designing hybridization-based fluorescent probes based on natural nucleic acids.[9,47] However, acute enzyme degradation, high false-positive signals, potential immunotoxicity, and the need for delivery systems hampered their clinical translation. Despite the introduction of chemically modified nucleic acid analogs in the development of probes, the study of chemically modified nucleic acid-based miRNA detection techniques is still limited.[12]

Recently, TNA has been considered as a potential progenitor of RNA. TNA is made up of a backbone repeat of unnatural 4-carbon threose sugar, with phosphodiester linkages taking place at the 2′- and 3′-vicinal positions of the threofuranose ring.[22,32] Recently, we have reported a cost-efficient approach to synthesize TNA phosphoramidite monomers and sequence-designed TNA polymers at high synthetic yield and purity. We found that these sequence-controlled, synthetic TNA polymers are able to form stable duplex Watson-Crick antiparallel structures and show strong specificity and affinity toward their complementary DNAs, or RNAs. These synthetic TNA molecules are also alternatives to traditional antisense materials for target gene suppression and tumor growth inhibition *in vivo*, with no adverse toxicity.[28,37] Importantly, we found that these designed TNA polymers exhibit remarkable stability in FBS, human blood serum, pH extremes, and even under storage at room temperature for a few months. Other research groups also demonstrated applications of TNA in aptamer and XNAzyme development, gene regulation and therapeutics, and information storage.[35,40] These exceptional properties, and findings with regard to TNAs, fuel prospects for constructing biosensors composed of TNA-modified nucleotides to rival biosensors composed of conventional RNA or DNA backbones for disease biomarker detection.

In this study, we successfully developed TNA-based probes for rapid and accurate target miRNA detection and imaging in living cells. To the best of our knowledge, this is the first time that hybridization-based probes have been developed that leverage the base-pairing capability of TNA to natural nucleic acids for target miRNA detection. Based on the high binding specificity and affinity of TNAs to their complementary RNA sequences,[22,23] a strand displacement reaction would definitely occur upon the binding of the longer miRNA targets to the partially hybridized TNA strand in TNA probes. This process would result in a fluorescence enhancement as an output signal. Compared with previously reported nucleic acid-based probes, miRNA detection duration of this TNA probe is relatively short, while scrambled TNA

probes had a negligible response.[6,48–51] In addition, the TNA probes not only exhibit insignificant responses to non-target miRNAs, but also are able to distinguish target miRNAs with one to two base mismatches. These findings suggest the excellent specificity and sensitivity of TNA probes for miRNA detection.

Biological stability is always a major concern when applying nucleic acid-based probes for miRNA detection and imaging in living systems as it is a critical parameter to achieve high efficacy under physiological conditions.[33] In this study, the TNA probes avoid degradation when incubated with nuclease for 24 h, and are functionally intact after incubation at 40°C, which is even higher than the physiological temperature. These findings indicate that TNA probes are a more superior choice for cellular and *in vivo* assays over DNA probes. In addition, the TNA probes maintain their capability of rapid and accurate miRNA sensing after incubation at 4°C up to 7 days. The excellent storage stability, together with superior nuclease resistance and thermal stability, make TNA probes a promising candidate for long-term cellular or animal studies.[32,41] Our cellular studies indicate that our TNA probes can distinguish different expression levels of target miRNAs between positive and negative cell lines by distinct brightness of the fluorescence signals. Compared with HEK293 cells, the upregulation expression of miR-21 in HeLa cells is more obvious. Importantly, we demonstrate that these TNA probes cannot only sense and quantitatively image dynamic expression of tumor-related miRNAs in cancer cell lines, but can also be utilized for differentiation of different cell lines, which is a major goal in the field of live cell analysis.

In summary, we developed TNA-based probes for rapid and sensitive miRNA detection and imaging in living cells. Our TNA probes are highly specific and selective toward target miRNA, and are able to distinguish one or two base mismatches in target RNA molecules. Compared with DNA probes, our newly designed TNA probes have good nuclease stability, thermal stability, and exceptional storage ability for long-term cellular studies. In addition, TNA probes could be efficiently taken up by living cells with negligible cytotoxicity for dynamic real-time monitoring of target miRNAs. Importantly, the TNA probes could differentiate the distinct target miRNA expression levels in various cancer cell lines. This work presents the first attempt to use TNA oligonucleotides to fabricate a biologically stable and cost-effective biosensor for target miRNA detection and intracellular imaging, and to advance the future development and application of TNA molecules for biological and biomedical research.

MATERIALS AND METHODS

Materials

All chemicals and reagents were used as received without any further purification unless indicated. Tris(hydroxylmethyl)aminomethane, glycine, sodium dodecyl sulfate, ammonium persulfate, N,N,N′,N′-tetramethylethylenediamine, dimethyl sulfoxide (DMSO), StainsAll, ammonium hydroxide, MTT, and Hoechst 33258 stain solution were purchased from Sigma-Aldrich. FBS, Dulbecco's modified Eagle medium, PBS, penicillin-streptomycin solution, and trypsin were purchased from Invitrogen. Forty percent acrylamide/bis-acrylamide solution (19:1) was purchased from Bio-Rad. Modified controlled pore glass (1,000 Å), 1-[(2-cyanoethyl)-(N,N-diisopropyl)]-phosphoramidite, and other chemicals used for TNA synthesis were purchased from BioAutomation. Sephadex G-25 (DNA grade) was purchased from Amersham Biosciences. All TNA and DNA oligonucleotides used in this study were synthesized in our lab. The RNA oligonucleotides were purchased from Sangon Biotech. The sequences of all oligonucleotide strands are shown in Table S1. Ultrapure H_2O was used throughout this study.

Chemical synthesis and characterization of TNA polymers

Automated solid-phase chemical synthesis of TNA polymers was conducted with a BioAutomation MerMade MM6 DNA synthesizer as reported previously.[28] The detailed procedure is provided in the supplemental information as shown in Figure S1. After the synthesis, the TNA strands were purified via a standard gel extraction method. MALDI-TOF analysis and 15% denaturing PAGE analysis were performed to confirm synthesis of the sequence-specified TNA polymers. Denaturing PAGE was performed in 1× TBE buffer with a current of 30 mA at room temperature for 1 h. Quantification of TNA and DNA was carried by UV-vis analysis.

Strand displacement reaction in TNA duplexes

TNA duplexes were prepared by mixing TRSs (1.5 μg) and complementary Cy3-TSSs in a molar ratio of 1:1 and subsequent processing with a heating-cooling procedure from 95°C to 4°C. Afterward, miR-21 mimics (DNA) were added into the TNA duplexes and the solution was then incubated at 37°C for 40 min. The samples were then investigated by 12% native PAGE analysis. Native PAGE was performed in 1× TAMg buffer with a current of 30 mA for 6 h or 15 h at 4°C. After the electrophoresis, the gel was stained with StainAll and scanned for analysis. Gel scanning of Cy3 dye was conducted on a Fujifilm FLA-9000 scanner.

Optimization of experimental conditions

To refine the optimal sense strand length for miR-21 detection, the fluorescence intensity of TNA probes (500 nM) using various Cy3-TSSs (11, 13, and 15 bases) was measured. To refine the optimal time for miR-21 displacement reaction, the fluorescence intensity was monitored at designated time points (0, 1, 2, 5, 10, 20, and 40 min) after adding the miR-21. For all fluorescence experiments, the fluorescence intensity of Cy3 was excited at 534 nm and measured at 564 nm.

miR-21 detection in solution

The TNA-based probes (500 nM) in PBS buffer were incubated with target miR-21 at different concentrations (0, 1, 2, 5, 20, 50, 100, 200, 300, 400, 500, and 1,000 nM). After incubation for 40 min at 37°C, the fluorescence intensity was monitored. To evaluate the specificity, TNA-based probes were incubated with target miR-21 and three control miRNAs (miR-141, miR-143, and miR-429) at a concentration of 500 nM. To evaluate the sensitivity, TNA-based probes were incubated with target miR-21 and one (or two) base mismatched miR-21 at a concentration of 500 nM. The fluorescence intensity was

monitored after the incubation. All experiments were repeated three times.

Nuclease stability, thermal stability, and long-term storage stability

For the nuclease stability test, two sets of TNA-based probes (1 μM) were prepared in PBS buffer. FBS (10%) was added into only one set. All samples were then incubated at 37°C and the fluorescence intensity was monitored at designated time points (0, 1, 2, 4, 8, 12, and 24 h). After the fluorescence intensity measurements at each time point, 500 nM target miR-21 was added into the corresponding samples. After incubation, the fluorescence intensity was measured. The DNA-based probes were also tested for comparison.

For the thermal stability, TNA or DNA probes (500 nM) were prepared and incubated at designated temperatures (20°C, 30°C, and 40°C) for 40 min. After incubation, the fluorescence intensity was measured and analyzed.

To test long-term storage stability, TNA probes (500 nM) were prepared in PBS buffer and incubated at 4°C. The fluorescence intensity was monitored at designated time points (0, 1, 3, and 7 days). After the measurement of fluorescence intensity at each time point, target miR-21 was added into the corresponding samples. After incubation, the fluorescence intensity was measured.

FBS assay

Pure TNA or DNA probes were dissolved in PBS containing 10% FBS to obtain a final concentration of 0.15 μg/μL. Samples were then incubated at 37°C for various durations (0, 1, 2, 4, 8, 12, and 24 h). TNA or DNA samples without the addition of FBS in PBS were set as a control. Afterward, TNA and DNA samples were heated at 60°C for 20 min to denature enzymes. Samples were then characterized by 15% denaturing PAGE, stained with StainAll, and scanned for analysis and comparison. Denaturing PAGE was performed in 1× TBE buffer with a current of 30 mA at room temperature for 1 h.

Cytotoxicity assay

The cytotoxicity of TNA-based probes was assessed via standard MTT assays. HEK293 cells or HeLa cells were plated in 96-well plates at a density of 10,000 cells per well and incubated overnight at 37°C. Then, the medium was replaced with fresh medium containing TNA-based probes at different concentrations (0, 0.5, 1, 2, and 3 μM); the cells were then incubated for 24 or 48 h. Afterward, 20 μL MTT (5 mg/mL) in PBS buffer was added to each well. After incubation for an additional 4 h, the medium was discarded and 150 μL DMSO was added to each well. Plates were incubated at 37°C for 20 min, and the absorbance at 490 nm was measured on a Bio-Tek Cytation 3 microplate reader. The data are mean ± SD (n = 6).

Confocal fluorescence imaging

Confocal fluorescence imaging of HeLa cells was set as an example. Typically, HeLa cells were plated in 35-mm glass-bottomed dishes at a density of 150,000 cells per dish and incubated overnight at 37°C. The medium was replaced with medium containing TNA-based probes (100 nM) and cells were incubated for a further 24 h. Cells were washed three times with PBS buffer then fixed with 4% paraformaldehyde at room temperature for 15 min. Fixed cells were then washed three times with PBS buffer (pH 7.4). After PBS washing, the fixed cells were analyzed with a Leica TCS SP5 laser confocal scanning microscope. The excitation wavelength for the Cy3 dye was 514 nm, and the emission was collected at 550–600 nm.

Transfection

HeLa cells were plated in 35-mm glass-bottomed dishes at a density of 100,000 cells per dish. After incubation overnight at 37°C, anti-miR-21 strands were transfected into the cells in serum-free medium using Lipofectamine 3000 reagent (Invitrogen, Thermo Fisher Scientific) under the instructions to downregulate the miR-21 expression.

Statistics analysis

All data are presented as mean ± SD. Statistical analyses was performed using Student's t test where applicable.

SUPPLEMENTAL INFORMATION

Supplemental information can be found online at https://doi.org/10.1016/j.omtn.2021.12.040.

ACKNOWLEDGMENTS

This work was financially supported by The Science Technology and Innovation Committee of Shenzhen Municipality (JCYJ2019 0812160203619), National Science Foundation of China (21574109 and 21778043), the Health and Medical Research Fund (07181396 and 05160336), the Hong Kong Research Grants Council General Research Fund (11304719, 11301220, 11307421), and the City University of Hong Kong (9680104). We thank Dr. Jonathan Weng-Thim Ho for language editing and assistance with copy editing.

AUTHOR CONTRIBUTIONS

F.W. performed all solution and cellular experiments. L.S.L. synthesized the TNA oligonucleotides. P.L., H.M.L., and D.Y.T. assisted in the cell experiments. F.W. and P.K.L. conceived the study, analyzed the data, and prepared the figures. F.W. and P.K.L. wrote the manuscript with contributions from all authors. All authors reviewed and approved the manuscript.

DECLARATION OF INTEREST

P.K.L., F.W., and L.S.L. are listed as inventors on a US patent application by the City University of Hong Kong describing the preparation and use of TNA-based probes. The other authors declare no competing financial interests.

REFERENCES

1. Lee, R.C., Feinbaum, R.L., and Ambros, V. (1993). The *C. elegans* heterochronic gene Lin-4 encodes small RNAs with antisense complementarity to Lin-14. Cell *75*, 843–854.

2. Bushati, N., and Cohen, S.M. (2007). MicroRNA functions. Annu. Rev. Cell. Dev. Biol. *23*, 175–205.

3. Di Leva, G., and Croce, C.M. (2013). miRNA profiling of cancer. Curr. Opin. Genet. Dev. *23*, 3–11.
4. Dong, H.F., Lei, J.P., Ding, L., Wen, Y.Q., Ju, H.X., and Zhang, X.J. (2013). MicroRNA: function, detection, and bioanalysis. Chem. Rev. *113*, 6207–6233.
5. Tian, T., Wang, J.Q., and Zhou, X. (2015). A review: microRNA detection methods. Org. Biomol. Chem. *13*, 2226–2238.
6. Liu, J., Cui, M.R., Zhou, H., and Yang, W.R. (2017). DNAzyme based nanomachine for in situ detection of microRNA in living cells. ACS Sens. *2*, 1847–1853.
7. Yang, L.M., Liu, B., Wang, M.M., Li, J., Pan, W., Gao, X.N., Li, N., and Tang, B. (2018). A highly sensitive strategy for fluorescence imaging of microRNA in living cells and in vivo based on graphene oxide-enhanced signal molecules quenching of molecular beacon. ACS Appl. Mater. Interfaces *10*, 6982–6990.
8. Du, Y., and Dong, S.J. (2017). Nucleic acid biosensors: recent advances and perspectives. Anal. Chem. *89*, 189–215.
9. Samanta, D., Ebrahimi, S.B., and Mirkin, C.A. (2020). Nucleic-acid structures as intracellular probes for live cells. Adv. Mater. *32*, 1901743.
10. Santangelo, P.J., Nix, B., Tsourkas, A., and Bao, G. (2004). Dual FRET molecular beacons for mRNA detection in living cells. Nucleic Acids Res. *32*, 57.
11. Kohler, O., Venkatrao, D., Jarikote, D.V., and Seitz, O. (2005). Forced intercalation probes (FIT probes): thiazole orange as a fluorescent base in peptide nucleic acids for homogeneous single-nucleotide-polymorphism detection. Chembiochem *6*, 69–77.
12. Wang, Q., Chen, L., Long, Y.T., Tian, H., and Wu, J.C. (2013). Molecular beacons of xeno-nucleic acid for detecting nucleic acid. Theranostics *3*, 395–408.
13. Molenaar, C., Marras, S.A., Slats, J.C.M., Truffert, J.C., Lemaitre, M., Raap, A.K., Dirks, R.W., and Tanke, H.J. (2001). Linear 2'O-methyl RNA probes for the visualization of RNA in living cells. Nucleic Acids Res. *29*, 89.
14. Liu, L.S., Wang, F., Ge, Y.H., and Lo, P.K. (2021). Recent developments in aptasensors for diagnostic applications. ACS Appl. Mater. Interfaces *13*, 9329–9358.
15. Valoczi, A., Hornyik, C., Varga, N., Burgyan, J., Kauppinen, S., and Havelda, Z. (2004). Sensitive and specific detection of microRNAs by northern blot analysis using LNA-modified oligonucleotide probes. Nucleic Acids Res. *32*, 175.
16. Socher, E., Bethge, L., Knoll, A., Jungnick, N., Herrmann, A., and Seitz, O. (2008). Low-noise stemless PNA beacons for sensitive DNA and RNA detection. Angew. Chem. Int. Ed. Engl. *47*, 9555–9559.
17. Sun, H.B., Kong, J.M., Wang, Q.W., Liu, Q.R., and Zhang, X.J. (2019). Dual signal amplification by eATRP and DNA-templated silver nanoparticles for ultrasensitive electrochemical detection of nucleic acids. ACS Appl. Mater. Interfaces *11*, 27568–27573.
18. Briones, C., and Moreno, M. (2012). Applications of peptide nucleic acids (PNAs) and locked nucleic acids (LNAs) in biosensor development. Anal. Bioanal. Chem. *402*, 3071–3089.
19. Schoning, K.U., Scholz, P., Guntha, S., Wu, X., Krishnamurthy, R., and Eschenmoser, A. (2000). Chemical etiology of nucleic acid structure: the alpha-threofuranosyl-(3'→2') oligonucleotide system. Science *290*, 1347–1351.
20. Wilds, C.J., Wawrzak, Z., Krishnamurthy, R., Eschenmoser, A., and Egli, M. (2002). Crystal structure of a B-form DNA duplex containing (L)-alpha-threofuranosyl (3'→2') nucleosides: a four-carbon sugar is easily accommodated into the backbone of DNA. J. Am. Chem. Soc. *124*, 13716–13721.
21. Pinheiro, V.B., and Holliger, P. (2012). The XNA world: progress towards replication and evolution of synthetic genetic polymers. Curr. Opin. Chem. Biol. *16*, 245–252.
22. Yu, H.Y., Zhang, S., and Chaput, J.C. (2012). Darwinian evolution of an alternative genetic system provides support for TNA as an RNA progenitor. Nat. Chem. *4*, 183–187.
23. Pallan, P.S., Wilds, C.J., Wawrzak, Z., Krishnamurthy, R., Eschenmoser, A., and Egli, M. (2003). Why does TNA cross-pair more strongly with RNA than with DNA? An answer from X-ray analysis. Angew. Chem. Int. Ed. Engl. *42*, 5893–5895.
24. Yang, Y.W., Zhang, S., McCullum, E.O., and Chaput, J.C. (2007). Experimental evidence that GNA and TNA were not sequential polymers in the prebiotic evolution of RNA. J. Mol. Evol. *65*, 289–295.
25. Chaput, J.C., and Szostak, J.W. (2003). TNA synthesis by DNA polymerases. J. Am. Chem. Soc. *125*, 9274–9275.
26. Ichida, J.K., Zou, K., Horhota, A., Yu, B., McLaughlin, L.W., and Szostak, J.W. (2005). An in vitro selection system for TNA. J. Am. Chem. Soc. *127*, 2802–2803.
27. Sau, S.P., Fahmi, N.E., Liao, J.Y., Bala, S., and Chaput, J.C. (2016). A scalable synthesis of alpha-L-threose nucleic acid monomers. J. Org. Chem. *81*, 2302–2307.
28. Liu, L.S., Leung, H.M., Tam, D.Y., Lo, T.W., Wong, S.W., and Lo, P.K. (2018). Alpha-L-threose nucleic acids as biocompatible antisense oligonucleotides for suppressing gene expression in living cells. ACS Appl. Mater. Interfaces *10*, 9736–9743.
29. Mei, H., Liao, J.Y., Jimenez, R.M., Wang, Y.J., Bala, S., McCloskey, C., Switzer, C., and Chaput, J.C. (2018). Synthesis and evolution of a threose nucleic acid aptamer bearing 7-deaza-7-substituted guanosine residues. J. Am. Chem. Soc. *140*, 5706–5713.
30. Zhang, L., and Chaput, J.C. (2020). In vitro selection of an ATP-binding TNA aptamer. Molecules *25*, 4194.
31. Rangel, A.E., Chen, Z., Ayele, T.M., and Heemstra, J.M. (2018). In vitro selection of an XNA aptamer capable of small-molecule recognition. Nucleic Acids Res. *46*, 8057–8068.
32. Dunn, M.R., McCloskey, C.M., Buckley, P., Rhea, K., and Chaput, J.C. (2020). Generating biologically stable TNA aptamers that function with high affinity and thermal stability. J. Am. Chem. Soc. *142*, 7721–7724.
33. Wang, Y.J., Nguyen, K., Spitale, R.C., and Chaput, J.C. (2021). A biologically stable DNAzyme that efficiently silences gene expression in cells. Nat. Chem. *13*, 319–326.
34. Nguyen, K., Wang, Y.J., England, W.E., Chaput, J.C., and Spitale, R.C. (2021). Allele-specific RNA knockdown with a biologically stable and catalytically efficient XNAzyme. J. Am. Chem. Soc. *143*, 4519–4523.
35. Wang, Y., Wang, Y., Song, D., Sun, X., Zhang, Z., Li, X., Li, Z., and Yu, H. (2021). A threose nucleic acid enzyme with RNA Ligase activity. J. Am. Chem. Soc. *143*, 8154–8163.
36. Lange, M.J., Burke, D.H., and Chaput, J.C. (2019). Activation of innate immune responses by a cytosine-phosphate-guanine oligonucleotide sequence composed entirely of threose nucleic acid. Nucleic Acid Ther. *29*, 51–59.
37. Wang, F., Liu, L.S., Lau, C.H., Han Chang, T.J., Tam, D.Y., Leung, H.M., Tin, C., and Lo, P.K. (2019). Synthetic α-L-threose nucleic acids targeting BcL-2 show gene silencing and in vivo antitumor activity for cancer therapy. ACS Appl. Mater. Interfaces *11*, 38510–38518.
38. Li, X.T., Li, Z., and Yu, H.Y. (2020). Selection of threose nucleic acid aptamers to block PD-1/PD-L1 interaction for cancer immunotherapy. Chem. Commun. *56*, 14653–14656.
39. Lu, X.H., Wu, X.H., Wu, T.T., Han, L., Liu, J.B., and Ding, B.Q. (2020). Efficient construction of a stable linear gene based on a TNA loop modified primer pair for gene delivery. Chem. Commun. *56*, 9894–9897.
40. Yang, K.F., McCloskey, C.M., and Chaput, J.C. (2020). Reading and writing digital information in TNA. ACS Synth. Biol. *9*, 2936–2942.
41. Culbertson, M.C., Temburnikar, K.W., Sau, S.P., Liao, J.Y., Bala, S., and Chaput, J.C. (2016). Evaluating TNA stability under simulated physiological conditions. Bioorg. Med. Chem. Lett. *26*, 2418–2421.
42. Iorio, M.V., Ferracin, M., Liu, C.G., Veronese, A., Spizzo, R., Sabbioni, S., Magri, E., Pedriali, M., Fabbri, M., Campiglio, M., et al. (2005). MicroRNA gene expression deregulation in human breast cancer. Cancer Res. *65*, 7065–7070.
43. Zhu, D.B., Zhang, L., Ma, W.G., Lu, S.Q., and Xing, X.B. (2015). Detection of microRNA in clinical tumor samples by isothermal enzyme-free amplification and label-free graphene oxide-based SYBR Green I fluorescence platform. Biosens. Bioelectron. *65*, 152–158.
44. Liu, Y., Shen, T., Li, J., Gong, H., Chen, C.Y., Chen, X.M., and Cai, C.Q. (2017). Ratiometric fluorescence sensor for the microRNA determination by catalyzed hairpin assembly. ACS Sens. *2*, 1430–1434.
45. Huang, D.J., Huang, Z.M., Xiao, H.Y., Wu, Z.K., Tang, L.J., and Jiang, J.H. (2018). Protein scaffolded DNA tetrads enable efficient delivery and ultrasensitive imaging

of miRNA through crosslinking hybridization chain reaction. Chem. Sci. *9*, 4892–4897.

46. Li, J., Cai, S.J., Zhou, B., Meng, X.X., Guo, Q.P., Yang, X.H., Huang, J., and Wang, K.M. (2020). Photocaged FRET nanoflares for intracellular microRNA imaging. Chem. Commun. *56*, 6126–6129.

47. Pan, W., Liu, B., Gao, X.N., Yu, Z.Z., Liu, X.H., Li, N., and Tang, B. (2018). A graphene-based fluorescent nanoprobe for simultaneous monitoring of miRNA and mRNA in living cells. Nanoscale *10*, 14264–14271.

48. Pan, W., Li, Y.L., Wang, M.M., Yang, H.J., Li, N., and Tang, B. (2016). FRET-based nanoprobes for simultaneous monitoring of multiple mRNAs in living cells using single wavelength excitation. Chem. Commun. *52*, 4569–4572.

49. He, X.W., Zeng, T., Li, Z., Wang, G.L., and Ma, N. (2016). Catalytic molecular imaging of microRNA in living cells by DNA-programmed nanoparticle disassembly. Angew. Chem. Int. Ed. Engl. *55*, 3073–3076.

50. Zhang, E., Zhang, Y., Zhang, X.B., Li, Y.Y., He, Y.L., Liu, Y., and Ju, H.X. (2020). A photo zipper locked DNA nanomachine with an internal standard for precise miRNA imaging in living cells. Chem. Sci. *11*, 6289–6296.

51. Liu, C., Hu, Y.L., Pan, Q.S., Yi, J.T., Zhang, J., He, M.M., He, M.Y., Chen, T.T., and Chu, X. (2019). A microRNA-triggered self-powered DNAzyme walker operating in living cells. Biosens. Bioelectron. *136*, 31–37.